Growth kinetics of nc-Si:H deposited at 200 °C by hot-wire chemical vapour deposition

C. J. Oliphant[1,2], C. J. Arendse[1,*], D. Knoesen[1], T. F. G. Muller[1], S. Prins[2] and G. F. Malgas[3]

[1] Department of Physics, University of the Western Cape, Private Bag X17, Bellville 7535, South Africa

[2] National Metrology Institute of South Africa, Private Bag X34, Lynwood Ridge, Pretoria 0040, South Africa

[3] CSIR National Centre for Nano-Structured Materials, P. O. Box 395, Pretoria 0001, South Africa

Abstract

We report on the growth kinetics of hydrogenated nanocrystalline silicon, with specific focus on the effects of the deposition time and hydrogen dilution on the nano-structural properties. The growth in the crystallite size, attributed to the coalescence of smaller nano-crystallites, is accompanied by a reduction in the compressive strain within the crystalline region and an improved ordering and reduction in the tensile stress in the amorphous network. These changes are intimately related to the band gap of the material. Surface diffusion determines the growth in the amorphous regime, whereas competing reactions between silicon etching by atomic hydrogen and precursor deposition govern the film growth at the high-dilution regime. The diffusion of hydrogen within the film controls the growth during the transition from amorphous to nanocrystalline silicon.

[*] Corresponding author: C. J. Arendse, Tel: +27 21 959 3473, Fax: +27 21 959 3474,

Email: cjarendse@uwc.ac.za

Keywords

Nanocrystalline silicon, Kinetics, Crystallinity, Strain, Band gap, Confinement

1. Introduction

Hydrogenated amorphous silicon (a-Si:H) is an important material in modern electronic devices such as solar cells and thin film transistors. Currently, the focus has shifted towards hydrogenated nanocrystalline silicon (nc-Si:H) as a possible replacement for a-Si:H, due to its unique properties, e.g. tailored optical band gap [1] and superior resistance to photo-induced degradation [2]. The growth process and structure-property relationship of nc-Si:H has been the centre of numerous studies, as they would assist in the enhancement of growth rates and film properties. A need also exist for developing the synthesis of device quality nc-Si:H at low substrate temperatures as it would promote the use of flexible substrates.

This contribution presents an investigation into the effects of hydrogen (H)-dilution and deposition time on the evolution of the nano-structural properties and the band gap of nc-Si:H synthesised by hot-wire chemical vapour deposition (HWCVD) at a substrate temperature of 200 °C. Subsequently, growth mechanisms are deduced from the observations for each H-dilution regime.

2. Experimental Details

The thin films were simultaneously deposited on single-side polished (100) crystalline silicon and Corning 7059 glass substrates using an ultra-high vacuum HWCVD system [3] from various

gas mixtures of SiH_4 and H_2. The H-dilution ratio, defined as $R = \frac{\Phi_{H_2}}{(\Phi_{H_2} + \Phi_{SiH_4})}$, where Φ denotes the gas flow rate, was varied from 80 – 95 %. At each *R*-value, varying the deposition time from 10 – 60 minutes enabled control over the film thickness. During all depositions, the filament temperature, deposition pressure, substrate temperature and total gas flow rate were fixed at 1600 °C, 60 μbar, 200 °C and 30 sccm, respectively.

The structural properties were investigated using a Jobin-Yvon HR800 micro-Raman spectrometer in backscattering geometry at room temperature in the region 100 – 1000 cm^{-1}, using an excitation wavelength of 514.5 nm. X-ray diffraction (XRD) was performed using a PANalytical Xpert diffractometer at 2θ-values ranging from 5 – 90°, with a step size of 0.02°. Copper $K\alpha_1$ radiation with a wavelength of 1.5406 Å was used as the x-ray source. Cross-sectional scanning electron microscopy (SEM) micrographs were recorded using a LEO 1525 field emission SEM. The film-thickness was determined using a Veeco® profilometer. Ultraviolet-visible (UV-VIS) spectra were measured in transmission mode from 200 – 900 nm using a Perkin-Elmer LAMDA 7505 UV/VIS spectrophotometer. The optical band gap was calculated using the method proposed by Swanepoel [4].

3. Results and Discussion

Presented in Fig. 1 (a) and (b) are the XRD spectra, highlighting the variations in the film crystallinity as a function of deposition time and H-dilution. After the first 10 minutes of deposition, the emergence of the Si (111) diffraction peak occurs at a H-dilution of 95%. After 60 minutes, the Si (111) diffraction peak is visible at *R*-values ≥ 83%. This suggests that the crystalline evolution, and hence the growth process, of nc-Si:H is dependent not only on the H-

dilution, but also on the deposition time. The enhancement of the Si (111) peak intensities and the reduction of its full-width-at-half-maximum (FWHM) with increasing H-dilution and deposition time indicate an increased crystalline volume fraction and a growth in the Si nano-crystallite size, respectively. The presence of lattice strain, nano-sized crystallites and instrumental effects are commonly the main contributors to the peak broadening in an XRD spectrum [5] and has generally been overlooked, especially for nc-Si:H [6]. For accurate quantitative analysis; a polycrystalline silicon and a NIST SRM 660 LaB_6 reference sample were used to obtain the corrected 2θ-peak position and the instrumental broadening, respectively. The crystallite size d_{XRD} of the Si (111)-peak was then calculated from the Scherrer formula, $d_{XRD} = \frac{0.9\lambda}{B_{structure}\cos\theta}$, where $B_{structure}$ is the structural broadening calculated from the measured FWHM of the raw spectrum and that of the LaB_6 reference by $B_{structure} = B_{measured} - B_{reference}$. The lattice strain ε was calculated from $B_{strain} = 4\varepsilon \tan\theta$, where $B^2_{strain} = B^2_{measured} - B^2_{reference}$ [5].

Presented in Fig. 1 (c) is the crystallite size-strain analysis of the Si (111) peak at different H-dilutions and deposition times. It is evident that the growth in crystallite size is associated with a reduction in the compressive strain of the Si crystallites. We propose that this behaviour is due to the coalescence of nano-crystallites, accompanied by the removal of strained Si-H bonds from the grain boundaries, and the nucleation of smaller crystallites, undetectable by XRD. This results in the growth of the crystallite size and an increase in the crystalline volume fraction. The cross-section scanning electron micrograph, shown in Fig. 1 (d), confirms the increase in the crystallite size and crystalline volume fraction as a function of deposition time, as evident by the conical growth.

Fig. 2 (a) and (b) compares the Raman spectra of the thin films deposited for 10 and 60 minutes at various H-dilutions. The spectra display the following main features: (i) a sharp peak centred around 516 cm^{-1}, associated with the transverse optic (TO) mode of the nc-Si phase; (ii) the broad shoulder centred around 480 cm^{-1}, due to the TO-mode of the amorphous silicon (a-Si) phase; and (iii) a smaller shoulder around 505 cm^{-1}, corresponding to the distribution of crystalline grain boundaries in the sample. The appearance of the nc-Si TO-peak at $R \geq 83$ % signals the nucleation of smaller Si nano-crystallites within the a-Si matrix after 10 minutes of deposition, which is undetectable with XRD. It should be noted that Raman spectroscopy is more sensitive to short-range order than XRD. The crystalline volume fraction, $f_c = [A_{505} + A_{516}]/[A_{505} + A_{516} + A_{480}]$, was estimated from the integrated areas of the afore-mentioned deconvoluted Gaussian peaks (505 cm^{-1} and 480 cm^{-1}) and a Lorentzian peak (516 cm^{-1}). The crystallite size is empirically determined from the shift of the nc-Si TO-peak relative to the bulk c-Si peak at 520 cm^{-1} [7]. Fig. 2 (c) and (d) show that the crystalline volume fraction increased and saturates after 20 minutes, while the crystallite size varied slightly (~ 1 nm) with increasing H-dilution and deposition time, which is contrary to previous studies [8]. Therefore, an increase in H-dilution and deposition time induces an enhanced nucleation rate of silicon nano-crystals with minimal effect on the average crystallite size. The increase in the crystallite size observed from XRD may therefore be attributed to the coalescence of smaller crystallites, resulting from the high crystalline volume fraction and increasing film thickness also reported by Wronski *et al.* [9].

The peak position of the a-Si TO-peak shifts to higher wavenumbers with an increase in H-dilution and time, which is indicative of an improvement in the ordering within the a-Si matrix and hence a reduction in the tensile strain [10]. This suggests that larger Si crystallites (> 12 nm) are under compressive stress, attributed to the surrounding a-Si network that is under tensile

stress. The combined effects of these two types of stresses then determine the total film stress [11]. Therefore the reduction in compressive strain in the Si nano-crystallites can be associated with an improvement in the ordering and a reduction in the tensile stress in the surrounding a-Si network. Tensile stress in nc-Si:H originates from the removal of H from grain boundaries, coalescence of crystallites and the presence of micropores [12], which are characteristic for these films [1].

The main factors that influence the band gap of nc-Si:H includes the quantum confinement effect due to the nano-crystallite size [1], film stress [13], hydrogen concentration and distribution, and microvoids [14]. Nonetheless, our results show that these factors are intimately linked in nc-Si:H thin films. Presented in Fig. 3 is the Tauc band gap as a function of deposition time and H-dilution. The band gap remains relatively constant for $R \leq 83$ % and then increases at higher H-dilutions, which can be ascribed to the quantum confinement effect via to the nucleation of smaller crystallites, difficult to detect with Raman and XRD. However, microvoids prevalent at higher H-dilutions reduce the density of the material and cause an increase in the average Si-Si distance, which also produces a high band gap [14]. The subsequent reduction of the band gap with longer deposition times is due to the growth in the Si crystallite size and the improved ordering and reduction in the stress within the film.

The XRD and Raman results reveal that the structural order of both the a-Si and nc-Si regions within the films varies with H-dilutions and deposition time, i.e. there may be different growth mechanisms at work depending on the deposition regime. Since the growth of nc-Si:H are governed by reactions at the substrate, plotting the film thickness (d_f) as a function of time at different H-dilutions can reveal if the growth process is surface controlled or diffusion controlled. Fig. 4 shows the film thickness as a function of deposition time at various H-

dilutions. A linear growth rate occurs at R = 80 and 95 %, which suggests that the reactions at the surface of the thin film controls film growth within this regime. Conversely, when the film undergoes transformation from a-Si:H to nc-Si:H (R = 83 – 90%) the growth follows a parabolic law, suggesting a diffusion-based growth.

Three schools of thought have been receiving the most attention to date for a possible growth mechanism, i.e. the atomic hydrogen (H^o)-etching model [15], the surface diffusion [16] and the chemical annealing model [17]. The H^o-etching model entails the selective etching of the a-Si phase by H^o, while the surface reaction models suggest an increased mobility of Si-containing radicals on a H-terminated surface until it finds energetically favourable sites to grow. The chemical annealing model claims that exothermic recombination of H^o to from molecular hydrogen (H_2) and the insertion of H into strained bonds serves as energy for the rearrangement of the Si-network or crystal nucleation. Yang *et al.* [18] performed *in situ* spectroscopic ellipsometry to analyze the microstructure of an a-Si:H / microcrystalline silicon (μc-Si:H) interface. They found that H^o penetrates the surface of the a-Si:H layer and increases its H-content. Subsequently, a μc-Si:H layer nucleates on top of a high H-content a-Si:H layer. The μc-Si:H layer then grows at the expense of the underlying high H-content a-Si:H layer. Reduced levels of H-coverage on the surface and the low substrate temperature suggests that the surface diffusion of Si-species may determine the growth at R = 80 %. Increasing the H-dilution ratio to 83 – 90% implies an increase in the H^o concentration, subsequently leading to the diffusion of H^o into the a-Si:H network where reconstruction and ordering occurs. This leads to the in-diffusion of H as being the governing factor in film growth at these conditions. At 95 %, extreme levels of H^o-etching cause a porous structure that persists throughout the first 60 minutes of deposition. In conjunction with a superior flux of H^o, competing rates of H^o-etching and Si deposition at the surface becomes the dominating step for film growth at this regime of deposition.

4. Conclusion

The growth process of nc-Si:H during HWCVD was interpreted in detail as a function of deposition time and H-dilution. XRD and Raman analyses showed that larger crystallites are under compressive stress induced by the surrounding a-Si:H network. The variation in the band gap energy was accounted for by the strain and crystallite size. At R = 80 % the film growth was determined by surface diffusion of growth species, while at R = 95 % the growth was due to competing H^o-etching effects and Si deposition. The growth-controlling step at the transition regime was determined to the diffusion of H^o within the film.

Acknowledgements

The authors acknowledge the financial support of the National Research Foundation and the National Metrology Institute of South Africa (Project no: TP 021). The authors are especially thankful to Mr. David Motaung for the valuable assistance with the XRD and Raman measurements. Ms. N. Nel-Sakharova and Mr. R. Pepenene are gratefully acknowledged for assisting with the UV-VIS measurements.

References

1. J. Kitao, H. Harada, N. Yoshida, Y. Kasuya, M. Nishio, T. Sakamoto, T. Itoh, S. Nonomura, Sol. Energy Mater. Sol. Cells 66 (2001) 245.
2. V. Shah, J. Meier, E. Vallat-Sauvain, N. Wyrsch, U. Kroll, C. Droz, U. Graf, Sol. Energy Mater. Sol. Cells 78 (2003) 469.
3. C.J. Arendse, G.F. Malgas, T.F.G. Muller, D. Knoesen, C.J. Oliphant, D.E. Motaung, S. Halindintwali, B.W. Mwakikunga, Nanoscale Res. Lett. 4 (2009) 307.
4. R. Swanepoel, J. Phys. E. Sci. Instrum. 16 (1983) 1214.
5. H.P. Klug, L.E. Alexander, X-Ray Diffraction Procedures for Polycrystalline and Amorphous Materials 2nd edition, Wiley-Interscience Publication, 1974.
6. B.P. Swain. South African J. Science 105 (2009) 77.
7. Y. He, C. Yin, G. Cheng, L. Wang, X. Liu, G.Y. Hu, J. Appl. Phys. 75 (1994) 797.
8. P. Gogoi, P. Agarwal, Sol. Energy Mater. Sol. Cells 93 (2009) 199.
9. C.R. Wronski, B. Von Roedernb, A. Kołodziej, Vacuum 82 (2008) 1145.
10. I. de Wolf, Semicond. Sci. Technol. 11 (1996) 139.
11. J.P. Conde, P. Alpium, M. Boucinha, J. Gaspar, V. Chu, Thin Solid Films 395 (2001) 105.
12. K.H. Jun, R. Carius, H. Stiebig, Phys. Rev. B 66 (2002) 115301.
13. A. M. Ali, J. Luminescence 126 (2007) 614.
14. K.F. Feenstra, R.E.I. Scgropp, W.F. van der Weg, J. Appl. Phys. 85 (1999) 6843.
15. C.C. Tsai, G.B. Anderson, R. Thompson, B. Wacker, J. Non-Cryst. Solids 114 (1989) 151.
16. A. Matsuda, J. Non-Cryst. Solids 59–60 (1983) 767.
17. K. Nakamura, K. Yoshida, S. Takeoka, I. Shimizu, Jpn. J. Appl. Phys. 34 (1995) 442.
18. Y.H. Yang, M. Katiyar, G.F. Feng, N. Maley, J.R. Abelson, J. Appl. Phys. 65 (1994) 1769.

List of table and figure captions

Fig. 1 XRD spectra of the samples deposited at different H-dilutions for (a) 10 minutes and (b) 60 minutes. (c) Cross-sectional SEM micrograph of the sample deposited at an H-dilution of 90% for 60 minutes. (d) Size-strain analyses of samples deposited at different H-dilutions and deposition times.

Fig. 2 Raman spectra of the samples deposited at different H-dilutions for (a) 10 minutes and (b) 60 minutes. (c) Average crystallite size and (d) crystalline volume fraction of the samples as a function of H-dilution and deposition time.

Fig. 3 Band gap of the samples as a function of H-dilution and deposition time.

Fig. 4 Growth kinetics of the a-Si:H and nc-Si:H thin films at different H-dilutions.

Figure 1

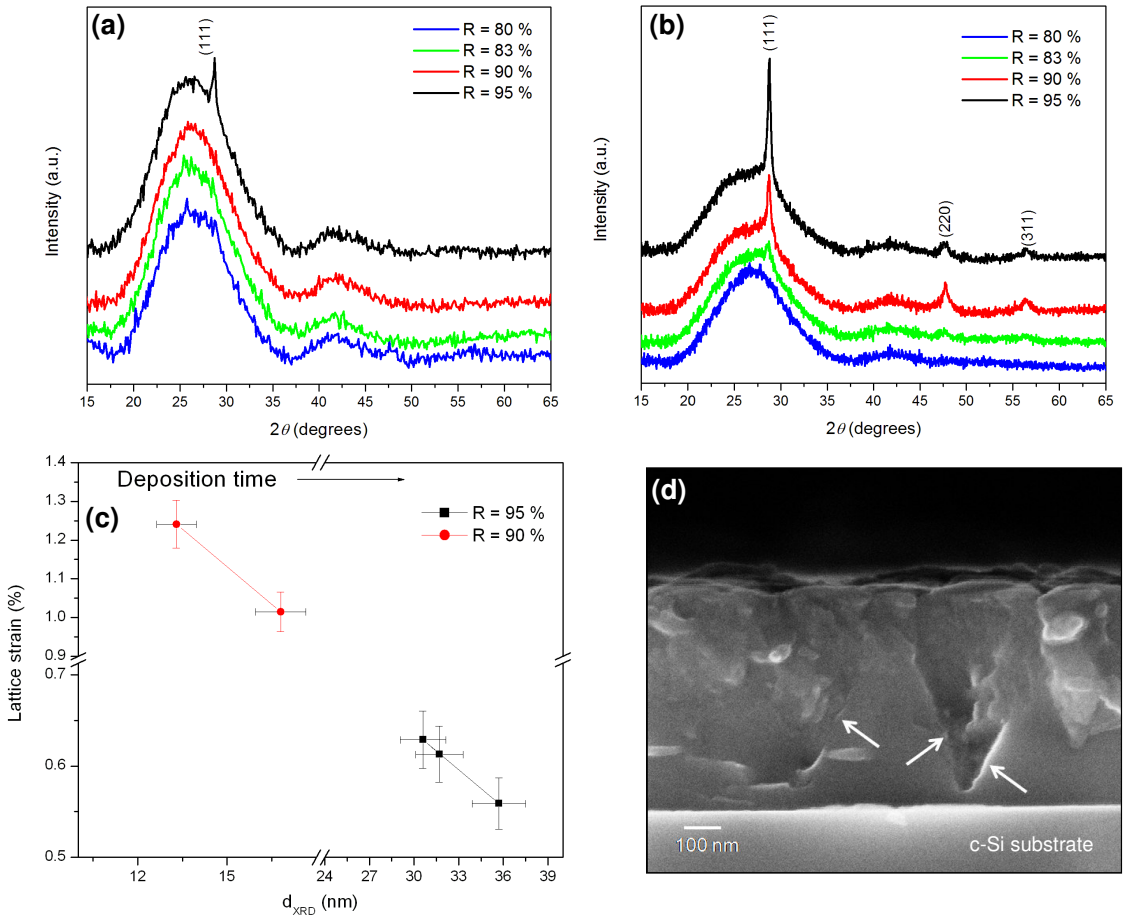
(a)
(111)
R = 80 %
R = 83 %
R = 90 %
R = 95 %
Intensity (a.u.)
2θ (degrees)
(b)
(111)
(220)
(311)
R = 80 %
R = 83 %
R = 90 %
R = 95 %
Intensity (a.u.)
2θ (degrees)
(c)
Deposition time
R = 95 %
R = 90 %
Lattice strain (%)
d_XRD (nm)
(d)
100 nm
c-Si substrate

Figure 2

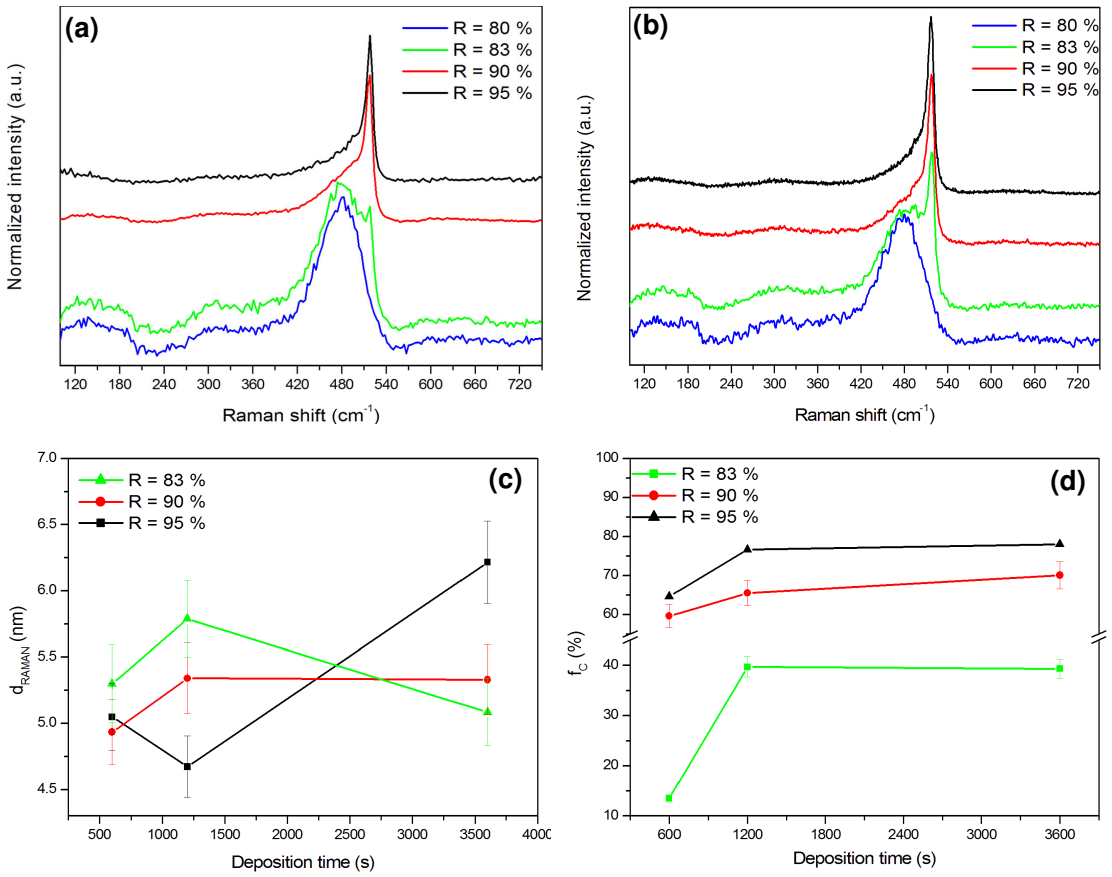
(a)
R = 80 %
R = 83 %
R = 90 %
R = 95 %
Normalized intensity (a.u.)
120 180 240 300 360 420 480 540 600 660 720
Raman shift (cm-1)
(b)
R = 80 %
R = 83 %
R = 90 %
R = 95 %
Normalized intensity (a.u.)
120 180 240 300 360 420 480 540 600 660 720
Raman shift (cm-1)
(c)
R = 83 %
R = 90 %
R = 95 %
dRAMAN (nm)
7.0 6.5 6.0 5.5 5.0 4.5
500 1000 1500 2000 2500 3000 3500 4000
Deposition time (s)
(d)
R = 83 %
R = 90 %
R = 95 %
fC (%)
100 90 80 70 60 40 30 20 10
600 1200 1800 2400 3000 3600
Deposition time (s)

Figure 3

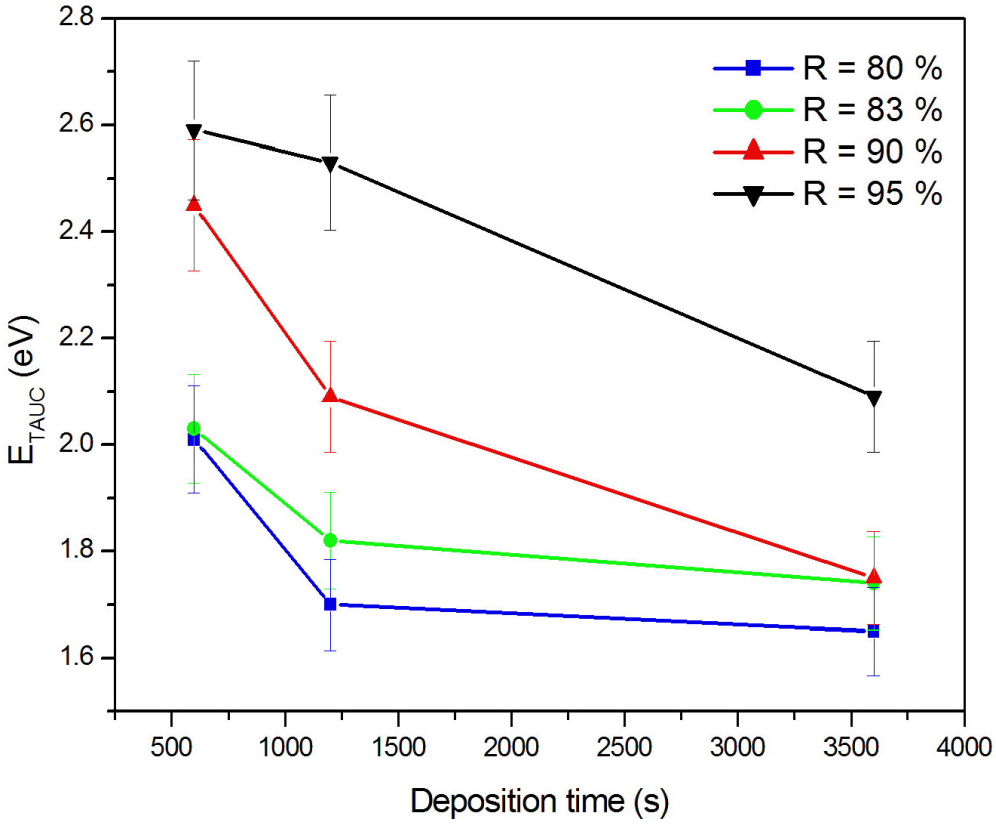
R = 80 %
R = 83 %
R = 90 %
R = 95 %
E_{TAUC} (eV)
Deposition time (s)
2.8
2.6
2.4
2.2
2.0
1.8
1.6
500
1000
1500
2000
2500
3000
3500
4000

Figure 4

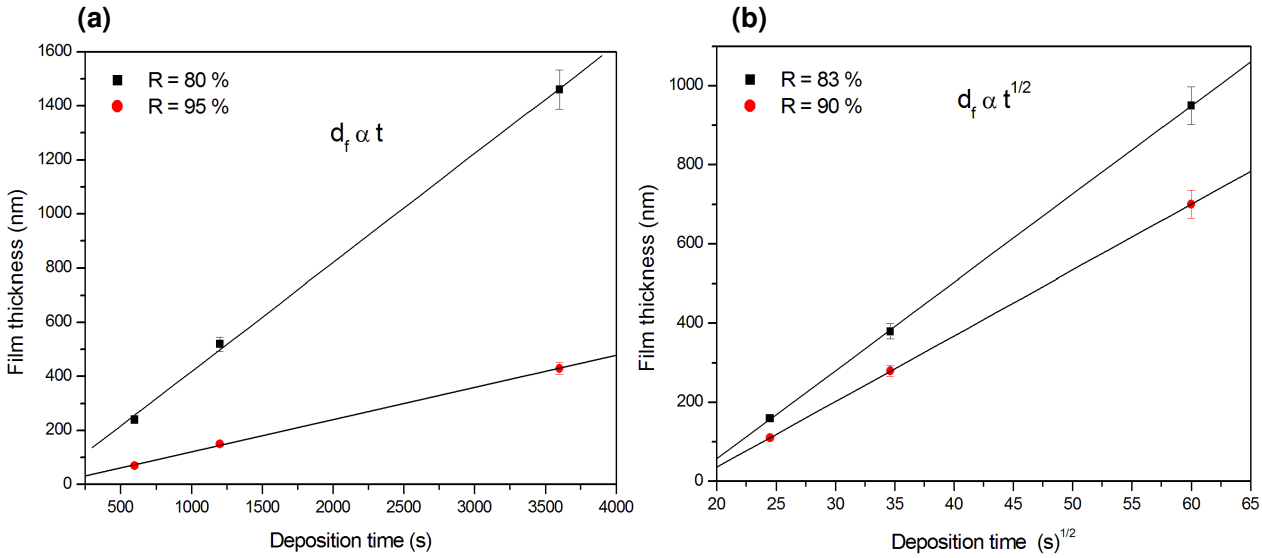
(a)
R = 80 %
R = 95 %
$d_f \alpha t$
Film thickness (nm)
Deposition time (s)
(b)
R = 83 %
R = 90 %
$d_f \alpha t^{1/2}$
Film thickness (nm)
Deposition time $(s)^{1/2}$